ScaleKD: Strong Vision Transformers Could Be Excellent Teachers

Jiawei Fan[*]
Intel Labs China
jiawei.fan@intel.com

Chao Li[*]
Intel Labs China
chao3.li@intel.com

Xiaolong Liu[*]
iMotion Automotive Technology
xiaolong.liu@imotion.ai

Anbang Yao[*†]
Intel Labs China
anbang.yao@intel.com

Abstract

In this paper, we question if well pre-trained vision transformer (ViT) models could be used as teachers that exhibit scalable properties to advance cross architecture knowledge distillation research, in the context of adopting mainstream large-scale visual recognition datasets for evaluation. To make this possible, our analysis underlines the importance of seeking effective strategies to align (1) feature computing paradigm differences, (2) model scale differences, and (3) knowledge density differences. By combining three closely coupled components namely *cross attention projector*, *dual-view feature mimicking* and *teacher parameter perception* tailored to address the alignment problems stated above, we present a simple and effective knowledge distillation method, called *ScaleKD*. Our method can train student backbones that span across a variety of convolutional neural network (CNN), multi-layer perceptron (MLP), and ViT architectures on image classification datasets, achieving state-of-the-art knowledge distillation performance. For instance, taking a well pre-trained Swin-L as the teacher model, our method gets 75.15%|82.03%|84.16%|78.63%|81.96%|83.93%|83.80%|85.53% top-1 accuracies for MobileNet-V1|ResNet-50|ConvNeXt-T|Mixer-S/16|Mixer-B/16|ViT-S/16|Swin-T|ViT-B/16 models trained on ImageNet-1K dataset from scratch, showing 3.05%|3.39%|2.02%|4.61%|5.52%|4.03%|2.62%|3.73% absolute gains to the individually trained counterparts. Intriguingly, when scaling up the size of teacher models or their pre-training datasets, our method showcases the desired scalable properties, bringing increasingly larger gains to student models. We also empirically show that the student backbones trained by our method transfer well on downstream MS-COCO and ADE20K datasets. More importantly, our method could be used as a more efficient alternative to the time-intensive pre-training paradigm for any target student model on large-scale datasets if a strong pre-trained ViT is available, reducing the amount of viewed training samples up to 195×. The code is available at `https://github.com/deep-optimization/ScaleKD`.

1 Introduction

Background. The great success of deep learning in computer vision (CV) has been driven by an explosion of neural network architectures among which convolutional neural networks (CNNs) [1–3], vision transformers (ViTs) [4, 5] and multi-layer perceptrons (MLPs) [6–8] are three major model categories. While CNNs were the de facto models for about a decade, recent progress shows that large ViT models have attained state-of-the-art performance on many visual recognition tasks such as image

[*] Core authors contributed to method formulation, experimental design and analysis.
[†] Corresponding author.

38th Conference on Neural Information Processing Systems (NeurIPS 2024).

https://doi.org/10.52202/079017-2022

classification, image segmentation, and object detection. In principle, ViTs extend the philosophy of predominant transformer architectures [9] in natural language processing (NLP) to vision tasks. They convert an image into a sequence of equal-sized patches treated as tokens resembling words in NLP, then apply the dot-product self-attention mechanism over the sequence of image patches. ViTs designed in this way couple with a powerful data-hungry learning paradigm: models are first pre-trained on massive datasets (with supervised or self-supervised [10, 11] or cross-modality learning [12, 13]) and then fine-tuned on target datasets (with supervised learning). As the size of ViT models or pre-training datasets increases, the pre-trained models tend to have improved generalization performance. Despite this notable model performance scalability, the pre-training process of ViTs leads to significantly huge expenses. Furthermore, large pre-trained ViTs are memory-hungry and computationally intensive, prohibiting their deployment in many resource-constrained application scenarios. In contrast, CNNs and MLPs are still widely used in industry, due to the wider availability of effective implementations and optimizations compared to ViTs.

Motivation of This Work. In parallel, knowledge distillation (KD) has proven to be a promising model compression pathway and has attracted lots of research interests. It relies on a teacher-student framework that transfers the knowledge learned by a large teacher model to a compact student model, aiming to make the student model can have improved performance to substitute the teacher model in deployment. However, most existing KD methods [14–35] focus on CNN architectures, and usually perform evaluation on small datasets with non-mainstream student models for industrial applications, lagging far behind the evolution of neural network architectures. Although there have been few recent efforts [36–39] on using ViT teachers, they explore narrow focuses that use small ViT teachers without pre-training on massive datasets, following the ways previously studied in CNN-based KD methods. In this paper, *we attempt to connect knowledge distillation research with well pre-trained ViT models that stand out for their remarkable scalability, via a new viewpoint*. Specifically, *we question* whether well pre-trained ViT models could be used as teachers that effectively transfer their scalable properties to target student models having different typed architectures such as CNN and MLP or heterogeneous ViT structures (we refer 'cross architecture KD' to such a more generalized formulation in this work), in the context of using mainstream large-scale visual recognition benchmarks.

Problem Analysis. To answer the question in our motivation, we think the knowledge transfer difficulties are rooted in the following three aspects of differences: (1) *Differences in feature computing paradigm*. In terms of semantic units, ViTs operate on a sequence of equal-sized image patches added with positional embeddings, whereas CNNs operate on regular grids of pixels. In terms of core operations, ViTs rely on self-attention operations to model global feature dependencies, whereas CNNs rely on convolution operations to model local features. Although MLPs also use a patchify stem as ViTs, they rely on fully connected operations instead of self-attention operations and do not use positional embeddings, showing inferior feature learning ability. These differences in feature computing paradigm pose the first knowledge transfer barrier to overcome. (2) *Differences in model scale*. On the micro scale, model scale differences among ViTs, CNNs, and MLPs lie in network width, network depth, building blocks, etc. On the macro scale, model scale differences come from the capability of scaling the model size for ViTs, CNNs and MLPs towards better performance and generalization ability. As a result, these differences in model scale make the capacity of different network architectures typically vary significantly, emerging as the second knowledge transfer barrier to address. (3) *Differences in knowledge density*. Under the prevalent pre-training and fine-tuning paradigm, when scaling up pre-training datasets, large ViTs usually exhibit obviously superior performance scalability than top-performing CNNs and MLPs in terms of fine-tuning on both upstream image classification tasks and downstream dense prediction tasks [40, 41]. As for knowledge distillation in this work, we assume that pre-training datasets are no longer accessible and only well pre-trained ViT teacher models are available, avoiding the expensive pre-training process and making the setting well suited for real applications. Under this context, when training student models on upstream image classification datasets like ImageNet-1K, the knowledge density between teacher and student models is different, which appears as the third barrier to handle. From the above analysis, we can conclude that the design of effective schemes to align (1) feature computing paradigm differences, (2) model scale differences, and (3) knowledge density differences between the pre-trained ViT teacher and target student models, plays the key role to attain our goal.

Design Insights and Contributions. Accordingly, we present Scalable Knowledge Distillation (ScaleKD), a simple and effective cross architecture KD method, which addresses the above difficulties in a progressive manner. Fundamentally, to bridge the feature computing paradigm differences

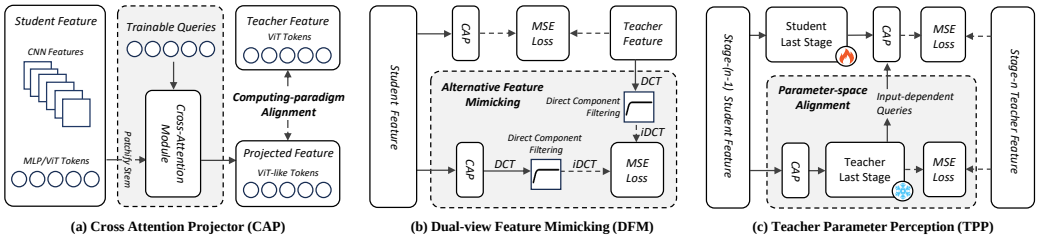

Figure 1: Overview of three core components in our ScaleKD, which are (a) cross attention projector, (b) dual-view feature mimicking, and (c) teacher parameter perception. Note that the teacher model is frozen in the distillation process and there is no modification to the student's model at inference.

between ViT and the other heterogeneous architectures, we propose *cross attention projector* (CAP, shown in Figure 1(a)), motivated by some previous works [42–44] that utilize cross attention mechanisms to align different modalities. For semantic unit differences, CAP utilizes positional embeddings and a patchify stem to transform the semantic units of CNN and MLP into transformer-like tokens. To further bridge core operation differences, CAP employs cross-attention operation and trainable queries that share the same attributes as the teacher's features to model global interdependencies on the student's features. In this way, CAP could align computing paradigm differences between the ViT teacher and the heterogeneous student in form, serving as the base component in our method.

Different from feature computing paradigm differences, model scale differences and knowledge density differences are not explicitly and separately modeled in the KD process, as they are intertwined under the prevailing pre-training and fine-tuning paradigm and are finally encoded in teacher and student models' feature space and parameter space. In light of this, we investigate both feature and parameter spaces of teacher and student models and observe two critical phenomena:

- **Feature Space:** As shown in Figure 2 and Figure 5, the frequency distributions of the features for the pre-trained ViTs are extremely imbalanced, where the direct component (zero frequency) response is dominant among all frequencies. This indicates that conducting feature distillation under such an imbalanced distribution may neglect the features of all other alternative components.
- **Parameter Space:** As the parameters of the pre-trained ViTs in the fine-tuning stage are slightly changed, their pre-training knowledge remains in the parameter space. Although the pre-training datasets are not accessible in this work, the student still has the opportunity to obtain the pre-training knowledge by aligning its parameter space to the teacher's.

Inspired by these two insightful observations, we formulate our method from two new perspectives. Based on the observation in feature space, we design *dual-view feature mimicking* (DFM, shown in Figure 1(b)), whose key insight is to complement the neglected alternative features in the KD process. Specifically, DFM employs CAP as the feature projector and incorporates two feature mimicking paths. In the first path, DFM conducts feature mimicking in the original space to learn the teacher's global features. In the second path, by removing the direct component in frequency space, DFM highlights the subtle alternative responses in feature mimicking, thus avoiding the neglect of these features. As a result, the two paths are complementary to each other, jointly promoting the feature space alignment. Based on the observation in parameter space, we propose *teacher parameter perception* (TPP, shown in Figure 1(c)), whose target is to transfer the pre-training knowledge by establishing a connection between teacher's and student's parameter spaces. Thanks to the aligned feature computing paradigm by CAP, TPP could bridge the student's early stages to the teacher's later stages and form a proxy feature processing path, where their parameter spaces join hands for KD optimization. By applying feature distillation in this path, the student's parameter space tends to be gradually aligned with the teacher's, and the pre-training knowledge would be transferred from the teacher to the student. Since the distillation learning processes in feature space and parameter space are the two sides of the same coin, DFM and TPP could naturally reinforce each other in essence.

Benefited from the progressive designs, CAP, DFM, and TPP can be seamlessly integrated into a neat and effective cross architecture knowledge distillation method, called *ScaleKD*, which addresses the above three problems as a whole. Although ScaleKD has multiple feature mimicking paths, they only exist in the training stage. That is, ScaleKD does not alter the student's structure and introduces no additional cost in the inference stage. By conducting systematic experiments on several mainstream large-scale vision benchmarks, we validate the effectiveness and generalization ability of our method.

https://doi.org/10.52202/079017-2022

2 Method

Given a pre-trained ViT teacher having m stages and a target student (CNN or MLP or ViT) having n stages, let F^{s_i} and F^{t_j} denote features from *i-th* stage of the student and *j-th* of the teacher, respectively. In what follows, we formulate all three components of ScaleKD in the form of performing feature distillation, for better clarifying their tightly coupled relationships.

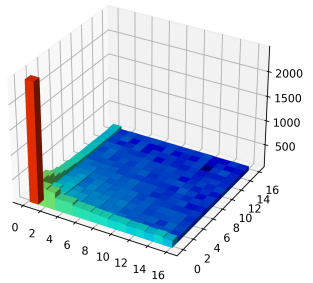

Figure 2: Feature distribution of BEiT-L/14 [41] in the frequency domain, where the direct component response is dominant. Details on drawing this figure are shown in Figure 5.

2.1 Three Core Components in ScaleKD

Cross Attention Projector. As shown in Figure 1(a), CAP adopts the structure of a standard transformer decoder block, consisting of a transformer decoder layer and an MLP layer, but incorporates three critical modifications. For brevity, taking CNN as an example, our modifications include: i) patchifying regular grids of pixels in CNN; ii) adding positional embeddings; iii) setting queries in the transformer decoder block as trainable variables that share the same resolution with the teacher's features. The first two modifications intend to narrow the discrepancy between different semantic units of the pre-trained ViT teacher and the CNN student, while the last modification endows the employed transformer decoder block with great flexibility to align feature semantics and spatial resolution. For MLP and ViT students, we adopt the same CAP structure as to CNN students for simple implementation but they can adapt CAP with fewer modifications when necessary. Based on these modifications, the cross-attention operation further models global dependencies on the projected student features. With CAP, the feature distillation loss is defined as:

$$\mathcal{L}_{CAP} = \alpha L(F^t, f_p(F^s; q)) = \alpha ||F^t - f_p(F^s; q)||_2^2, \tag{1}$$

where f_p, q, $\alpha(\geq 0)$, and $L(\cdot)$ denote the CAP, the trainable queries, the loss weight, and the L_2-normed distance, respectively.

Dual-view Feature Mimicking. As shown in Figure 1(b), building upon CAP, DFM contains two feature mimicking paths. As we stated in Section 1, the first path aims to learn the teacher's global features and the second path aims to excite and mimic the alternative features (neglected by existing KD methods). Specifically, in the first path, DFM conducts feature mimicking in the teacher's original feature space, which is formulated as: $\mathcal{L}_{ori} = \alpha L(F^t, f_{p_1}(F^s, q_1))$, where f_{p_1} and q_1 denote the CAP and its trainable queries in the first path, respectively. In the second path, the dominant direct component should be removed. To achieve this goal, we first employ discrete cosine transform (DCT), which maps the features from the spatial domain to the frequency domain: $DCT : \mathcal{X} \rightarrow \mathcal{Z}$. We then define an operator ϕ that removes direct component response from the features:

$$\phi(x) = DCT^{-1}(\sigma(DCT(x))) \qquad s.t.\ \sigma(z) = \begin{cases} 0, & z = 0 \\ z, & z \neq 0 \end{cases}. \tag{2}$$

Next, feature mimicking in the second path is formulated as: $\mathcal{L}_{alt} = \alpha L(\phi(F^t), \phi(f_{p_2}(F^s; q_2)))$, where f_{p_2} and q_2 denote the CAP and its trainable queries in the second path, respectively. Now, the feature distillation loss of DFM is formulated as:

$$\mathcal{L}_{DFM} = \beta \mathcal{L}_{ori} + (1 - \beta)\mathcal{L}_{alt}, \tag{3}$$

where $\beta \in [0, 1]$ denotes the balancing weight.

Teacher Parameter Perception. As we stated in Section 1, TPP establishes a proxy feature processing path by connecting the student's early stages to the teacher's later stages through a CAP. In our implementation, the proxy path consists of the student's first $n-1$ stages and the teacher's last stage, as illustrated in Figure 1(c). By feature mimicking in this proxy path, the parameters of the

https://doi.org/10.52202/079017-2022

student part are gradually aligned with the parameters of the teacher part, thus enabling the transfer of the teacher's pre-training knowledge. Let $F^{st} = g_{t_m}(f_p^{st}(F^{s_{n-1}}; q))$ be the output features of the proxy path, where g_{t_m} and f_p^{st} denote the teacher's last stage and the CAP in this path, respectively. The feature mimicking in the proxy path is formulated as: $\mathcal{L}^{st} = \alpha L(F^t, F^{st})$. We further introduce F^{st} as input-dependent queries for the CAP in the original path. This feature mimicking design aims to enhance the capability of CAP as such queries contain more teacher-related information, and its corresponding loss is formulated as $\mathcal{L}^s = \alpha L(F^t, f_p^s(F^{s_n}; F^{st}))$. With a simple principle of equal treatment to the two feature mimicking paths, the feature distillation loss of TPP is defined as:

$$\mathcal{L}^{TPP} = \mathcal{L}^s + \mathcal{L}^{st}. \tag{4}$$

2.2 Overall Formulation

From a general perspective, the progressive designs of our above three components are naturally coupled. As CAP serves as the basic component in DFM and TPP, we further introduce how to apply DFM in TPP and get a neat formulation of our method, ScaleKD. Specifically, if treating DFM as an improved version of traditional feature mimicking, it can substitute the original feature mimicking in each path of TPP. In this way, we formulate the overall design of ScaleKD, whose loss is defined as:

$$\mathcal{L}_{ScaleKD} = \mathcal{L}_{task} + \underbrace{\beta\mathcal{L}^s_{ori} + (1-\beta)\mathcal{L}^s_{alt}}_{\textit{DFM for TPP Student Path}} + \underbrace{\beta\mathcal{L}^{st}_{ori} + (1-\beta)\mathcal{L}^{st}_{alt}}_{\textit{DFM for TPP Teacher Path}} + \mathcal{L}_{kd}, \tag{5}$$

where $\beta \in [0, 1]$ is the balancing weight, $\mathcal{L}_{task}$ is the cross-entropy loss, and $\mathcal{L}_{kd}$ is the vanilla logits-based KD loss [14] widely used in previous KD research. As the features are standardized, we set $\alpha = 1$ for loss terms in DFM as the default. Hence, our method has only one hyper-parameter β.

3 Main Experiments

We perform comprehensive experiments to systematically validate the efficacy of our method and answer the question in our motivation. Specifically, our experimental verification contains six parts: i) validating the effectiveness of our method under basic settings; ii) conducting main experiments on ImageNet-1K [45] (IN-1K) dataset with various student backbones and showing the promising performance gains of our method against individually trained counterparts; iii) verifying whether our method could transfer the scalable properties of the teacher to the target student; iv) conducting transfer learning on downstream tasks with MS-COCO [46] and ADE20K [47] datasets to examine whether the performance gains from our method could be well preserved; v) comparing our method with recent top KD methods; vi) showing the potential impact of our method on model engineering.

Unless otherwise stated, in experiments, the student backbones are trained on IN-1K from scratch, without the pre-training on other upstream datasets. Experimental details are in Appendix A and B.

3.1 Pilot Experiments under Basic Settings

As we mentioned in Section 1, ScaleKD is tailored for: i) transferring the pre-trained ViT teacher's knowledge to the student having different model architectures; ii) making the student inherit the teacher's scalability. Therefore, we first perform the following two pilot experiments.

Cross Architecture Knowledge Distillation. To illustrate the difficulty of cross architecture feature distillation and validate the efficacy of ScaleKD under this setting, we compare ScaleKD with traditional feature distillation (FD) [15] on two different cross architecture teacher-student network pairs. From the results shown in Table 1, we can observe: i) due to architecture gaps between the teacher and the student, traditional FD shows limited performance gains; ii) comparatively, our ScaleKD achieves significantly better performance, bringing 2.75%|3.22% absolute top-1 gain for ResNet-50|Mixer-S. With the above experiments, we preliminarily verify that ScaleKD could effectively handle cross architecture feature distillation, which is difficult for traditional FD.

Large Pre-trained ViTs as Teachers. With ResNet-50 as the student, we examine the rationality of selecting large pre-trained ViTs as teachers in ScaleKD. Specifically, we gradually scale up the teacher's model capability (first from Swin-S to Swin-B, and then to Swin-L) and perform experiments

 https://doi.org/10.52202/079017-2022

Table 1: Pilot experiments on cross architecture distillation with ScaleKD and FD. s_i denotes the distillation is conducted on stage-i. To clearly show the performance gain, experiments in this table are conducted without L_{kd}.

Teacher	Student	Method	Top-1(%)	ΔTop-1(%)
Swin-S (83.02)	ResNet-50	*Baseline*	76.55	-
		FD (s_4)	77.43	+0.88
		FD (s_3,s_4)	77.74	+1.19
		ScaleKD	79.30	+2.75
	Mixer-S	*Baseline*	74.02	-
		FD (s_4)	74.88	+0.86
		FD (s_3,s_4)	75.32	+1.30
		ScaleKD	77.24	+3.22

Table 2: Pilot experiments on scaling up the teacher size. The advanced training strategy uses more sophisticated data augmentation and optimizer, and longer training epochs, as shown in Table 10.

Teacher	Student	Ratio of T/S Params	Top-1(%)	ΔTop-1(%)
ScaleKD with Traditional Training Strategy				
Baseline	ResNet-50	-	76.55	-
Swin-S (83.02)		1.94×	79.62	+3.07
Swin-B (85.16)		3.43×	79.80	+3.25
Swin-L (86.24)		7.68×	80.10	+3.55
ScaleKD with Advanced Training Strategy				
Baseline	ResNet-50	-	78.64	-
Swin-S (83.02)		1.94×	81.43	+2.79
Swin-B (85.16)		3.43×	81.77	+3.13
Swin-L (86.24)		7.68×	82.03	+3.39

Table 3: Main results of ScaleKD on **11** teacher-student network pairs. † denotes the model pre-trained on IN-22K [45] and ‡ denotes the model pre-trained by EVA [41], which has the learned knowledge of LAION-2B [48].

Teacher	Student	Params (M)		FLOPs (G)		Accuracy (%)	
		T	S	T	S	Top-1	ΔTop-1
Swin-L† (86.24)	MobileNet-V1 (72.10)	196.53	4.23	34.04	0.58	75.15	+3.05
	ResNet-50 (78.64)		25.56		4.12	82.03	+3.39
	ConvNeXt-T (82.14)		28.59		4.46	84.16	+2.02
	Mixer-S/16 (74.02)	196.53	18.53	34.04	3.78	78.63	+4.61
	Mixer-B/16 (76.44)		59.88		12.61	81.96	+5.52
	ViT-S/16 (79.90)	196.53	22.05	34.04	4.61	83.93	+4.03
	Swin-T (81.18)		28.29		4.36	83.80	+2.62
	ViT-B/16 (81.80)		86.57		17.58	85.53	+3.73
BEiT-L/14‡ (88.58)	ResNet-50 (78.64)	304.14	25.56	81.06	4.12	82.34	+3.70
	Mixer-B/14 (76.62)		59.88		16.45	82.89	+6.27
	ViT-B/14 (82.02)		86.57		23.09	86.43	+4.41

using two popular training strategies. From the results shown in Table 2, we can conclude: i) ScaleKD can help the student inherit the scalability of the teacher: it can be seen that the performance gain is consistently increased under both training strategies when scaling up the teacher's model size; ii) ScaleKD can adapt to teachers' training strategies: it can be seen that our ScaleKD always brings promising performance gains, although the baseline model under the advanced training strategy gets much more competitive performance than that under the traditional training strategy.

According to the above pilot experiments, *our ScaleKD shows basic capabilities on handling cross architecture knowledge distillation from large pre-trained ViTs to CNN and MLP students.*

3.2 Main Results

After verifying the effectiveness of our method under our basic settings, we move forward and perform extensive experiments on more teacher-student network pairs, in order to broadly examine the scalability of our method. Specifically, we construct **11** teacher-student network pairs by choosing **2** large teachers and **10** popular models for students, covering the current mainstream architectures across ViT, MLP, and CNN.

From the results shown in Table 3, we can observe: i) in general, our ScaleKD shows great generalization ability no matter for CNN, MLP and ViT students. Over 11 teacher-student pairs, the mean top-1 accuracy improvement reaches 3.94%, and the maximum is 6.27%; ii) considering the acceleration, with Swin-L as the teacher, ResNet-50|Mixer-S/16|ViT-S/16 trained by ScaleKD even outperforms individually trained ResNet-152|Mixer-B/16|ViT-B/16 by a margin of 0.28%|2.19%|2.13%, achieving over 2.35×|3.23×|3.83× compression in terms of model size; iii) the top-1 performance gain

Table 4: Experiments on exploring scalable properties from the teacher's pre-training data. We use the best reported models with different pre-training methods as our baselines to examine whether our student model has learned the teacher's pre-training knowledge. We use Swin-L as the teacher for the first two experiments and BEiT-L/14 as the teacher for the rest two experiments. $\Rightarrow$ denotes transfer learning and * denotes the model is trained and tested with 384$\times$ 384 sample resolution.

Model	Method	Training Dataset	Dataset Samples $\times$ Epochs (M)	Viewed Samples (M)	Top-1(%)
Supervised pre-training					
ViT-B/16	Pre-training [4]	IN-22K $\Rightarrow$ IN-1K	13.7$\times$90 + 1.28$\times$32	1274	83.97
		JFT-300M $\Rightarrow$ IN-1K	300$\times$7 + 1.28$\times$32	2141	84.15
	ScaleKD	IN-1K	1.28$\times$300	384	85.53
Self-supervised pre-training					
ViT-B/16	BEiT [40]	IN-22K $\Rightarrow$ IN-1K	13.7$\times$150 + 1.28$\times$100	2183	83.70
	iBOT [11]	IN-22K $\Rightarrow$ IN-1K	13.7$\times$320 + 1.28$\times$100	4512	84.40
	ScaleKD	IN-1K	1.28 $\times$ 300	384	85.64
Cross-modal pre-training					
ViT-B/16	CLIP [13]	LAION-2B $\Rightarrow$ IN-1K	2320$\times$32 + 1.28$\times$50	74304	85.47
		LAION-2B $\Rightarrow$ IN-12K $\Rightarrow$ IN-1K	2320$\times$32 + 12.1$\times$60 + 1.28$\times$50	75030	86.17
ViT-B/14	ScaleKD	IN-1K	1.28 $\times$ 300	384	86.43
EVA hybrid pre-training (MIM distillation from the cross-modal pre-trained teacher)					
EVA02-S/14*	EVA-02 [49]	IN-22K $\Rightarrow$ IN-1K	13.7$\times$240 + 1.28$\times$50	3352	85.80
	ScaleKD	IN-1K	1.28 $\times$ 300	384	86.22

Table 5: Transfer learning results (%) on MS-COCO.

Framework	Backbone	Pre-training	Classification (IN-1K)	Object Detection (COCO)				Instance Segmentation (COCO)			
			Top-1	AP	AP_S	AP_M	AP_L	AP	AP_S	AP_M	AP_L
Mask R-CNN	ResNet-50	*Baseline*	78.64	40.2	23.0	44.3	52.5	37.1	18.0	40.1	54.9
		Ours	82.03 (+3.39)	42.3	25.5	46.5	54.6	39.1	19.3	42.5	57.1
	Swin-T	*Baseline*	81.18	42.7	26.5	45.9	56.6	39.3	20.5	41.8	57.8
		Ours	83.80 (+2.62)	44.4	28.7	47.9	58.6	40.8	21.8	43.7	59.8

could be increased further, when choosing stronger teachers. For instance, ScaleKD brings 0.32% additional gain to ResNet-50 when changing the pre-trained ViT teacher from Swin-L to BEiT-L/14.

3.3 The Scalable Properties from Teacher's Pre-training Data

As we introduced in Section 1, the ViT's performance scalability is related to two factors: model scale and pre-training data scale. The experiments in Section 3.1 and 3.2 have validated that our method could help the student inherit the positive performance effect from increasing the teacher's model scale. In this subsection, we focus on exploring the second factor: *whether or not our method could help the student learn the teacher's pre-training knowledge from its massive pre-training datasets, mitigating the knowledge density gap.* To examine this, we alter our baselines to models with pre-training and propose an evaluation principle: given that only IN-1K is visible, if ScaleKD can help the student model achieve similar performance as models with upstream pre-training, the answer to the above question is *Yes*. With this principle, we design a series of experiments based on the selected teachers in Table 4: Swin-L having the pre-training knowledge of IN-22K and BEiT-L/14 having the pre-training knowledge of LAION-2B. We compare the performance of the student models trained by ScaleKD and the corresponding counterparts trained by prevailing pre-training methods.

From Table 4, we can observe that ScaleKD performs better than various pre-training methods across all four kinds. Note that the superior performance of ScaleKD is achieved conditioned on not viewing any pre-training data. In other words, ScaleKD merely views 5.58$\times$, 11.75$\times$, 195.39$\times$, and 8.73$\times$ less samples than the counterpart methods based on supervised pre-training, self-supervised pre-training, cross-modal pre-training, and hybrid pre-training. Therefore, we can summarize two promising conclusions: i) our method could help the student learn the teacher's pre-training knowledge from massive datasets and mitigate the knowledge density gap; ii) if a well pre-trained large ViT is available, our method can be a more efficient alternative to the time-intensive pre-training.

https://doi.org/10.52202/079017-2022

Table 7: Performance comparison with recent top-performing KD methods. Following the settings of them, the students are trained under the advanced training strategy. Best results are **bolded**.

Model	Method	Teacher	# Epochs	Top-1 (%)
Swin-T	From Scratch	-	300	81.18
	DIST [50]	**Swin-L (86.30)**	300	82.30
	DiffKD [51]	**Swin-L (86.30)**	300	82.50
	ScaleKD	Swin-L (86.24)	300	**83.80**
ResNet-50	From Scratch	-	300	78.60
	DIST[50]	Swin-L (86.30)	450	80.20
	DiffKD [51]	Swin-L (86.30)	450	80.50
	OFA [36]	**ViT-B (86.53)**	300	81.33
	ScaleKD	Swin-L (86.24)	300	**82.03**
	FunMatch [52]	BiT-Res152x2 (N/A)	1200	81.54
	FunMatch [52]	BiT-Res152x2 (N/A)	9600	82.31
	ScaleKD	Swin-L (86.24)	600	**82.55**

Table 8: Performance comparison with model engineering methods. More comparisons are shown in Table 14 in the Appendix.

Model	Params (M)	FLOPs (G)	Top-1 (%)
CNN-based Architecture			
ResNet-50 [2]	22.56	4.12	78.64
ResNet-50 + ScaleKD	22.56	4.12	82.55
ConvNext-T [3]	28.59	4.46	82.14
RepViT-2.3M [53]	22.90	-	82.50
MLP-based Architecture			
Mixer-B/16 [6]	59.88	12.61	76.44
Mixer-B/16 + ScaleKD	59.88	12.61	81.96
gMLP-B [8]	73.00	15.80	81.60
ResMLP-B24 [7]	115.7	23.00	81.00
ViT-based Architecture			
ViT-S/16 [4]	22.05	4.61	79.90
ViT-S/16 + ScaleKD	22.05	4.61	83.93
Swin-T [5]	73.00	15.80	81.18
Swin-B [5]	87.77	15.14	83.50

3.4 Transferring to Downstream Tasks

To further examine whether the performance gains from our method could be well preserved in transfer learning, we conduct comparative experiments on MS-COCO for object detection and instance segmentation, and on ADE20K for semantic segmentation.

Table 6: Transfer learning results (%) on ADE20K.

Framework	Backbone	Pre-training	IN-1K (Top-1)	ADE20K (mIOU)
UperNet	ResNet-50	*Baseline*	78.64	42.37
		Ours	82.03 (+3.39)	44.50 (+2.13)
	Swin-T	*Baseline*	81.18	44.41
		Ours	83.80 (+2.62)	46.33 (+1.92)
	ViT-B/16	*Baseline*	81.80	46.75
		Ours	85.53 (+3.73)	50.84 (+4.09)

The results on MS-COCO and ADE20K are shown in Table 5 and Table 6, respectively, from which we can observe: i) overall, our pre-trained models outperform their baselines by significant margins across three downstream tasks and different architectures; ii) for semantic segmentation on ADE20K, ViT-B/16 achieves the highest 4.09% absolute performance gain across three backbones, even higher than its gain on IN-1K; iii) for object detection and instance segmentation on MS-COCO, ResNet-50|Swin-T pre-trained by ScaleKD outperforms its baseline by an *AP* margin of 2.1%|1.7% and 2.0%|1.5%, respectively. The above observations illustrate that the performance gains from ScaleKD could be well transferred to various and challenging downstream tasks.

3.5 Comparison with Recent Top-Performing KD Methods

As we stated in Section 1 and 2, ScaleKD is a unified design incorporating three novel focuses to align computing paradigm differences, model scale differences, and knowledge density differences, which are clearly different from existing KD methods. In order to validate the superiority of our method, we compare ScaleKD with recent top-performing KD methods.

From the results shown in Table 7, we can see: i) compared to DIST, DiffKD and OFA, although our teacher is not the best and the number of training epochs is the smallest, our ScaleKD still outperforms the best of these methods by clear margins (0.70%|1.30% on ResNet-50|Swin-T); ii) compared to FunMatch, our method even shows superior performance, outperforming FunMatch by a margin of 0.24% but only using less than 10% training epochs. As a result, in the context of transferring the scalability of the pre-trained ViT to various student models, our systematic design and its focuses show obvious superiority to previous works, paving a new path for future KD research.

3.6 Potential Impact on Model Engineering

In Section 3.2, we have noticed ScaleKD brings significant performance gains to target students, especially for the plain design in each model category, such as ResNet, MLP-Mixer, and ViT. In parallel, model engineering is a common solution to improve the model performance. Considering these two facts, we conjure that since our method could bring competitive performance gain compared to model engineering, larger flexibility would be provided when choosing models in practice.

Table 9: Ablation studies. Experiments in (b)-(d) are performed on Swin-S→ResNet-50. As DFM and TPP are designed based on CAP, CAP is added by default when choosing DFM and TPP in (a). Because of this, we treat CAP as another baseline method, when analyzing DFM and TPP in (c)-(d).

(a) Ablation on the overall design

Teacher	Student	Ablation Design CAP	DFM	TPP	KD	Top-1
Swin-S	ResNet-50					76.55
		✓				77.87
		✓	✓			78.51
		✓		✓		78.62
		✓	✓	✓		79.30
		✓	✓	✓	✓	79.62
	Mixer-S					74.02
		✓				75.03
		✓	✓			76.42
		✓		✓		76.28
		✓	✓	✓		77.24
		✓	✓	✓	✓	77.59

(b) Ablation on CAP

Projector	Top-1	Δ Top-1
Baseline	76.55	-
Linear	77.43	+0.88
Conv	77.52	+0.97
CAP	77.87	+1.32

(c) Ablation on DFM

Feature Mimicking	Top-1	ΔTop-1
Baseline	76.55	-
CAP	77.87	+1.32
Dual-Path CAP	78.12	+1.57
DFM	78.51	+1.96

(d) Ablation on TPP

Method	TPP Design Proxy Path	Adaptive Queries	Accuracy (%) Top-1	ΔTop-1
Baseline	-	-	76.55	-
CAP	-	-	77.87	+1.32
TPP	✓	-	78.50	+1.95
TPP	✓	✓	78.62	+2.07

To study it, we apply ScaleKD to 3 standard designs of CNN, MLP and ViT, and compare the performance with recent advanced designs. From the results shown in Table 8, we observe that our method could help these models reach better performance than advanced models. More interestingly, in Table 3, we can clearly see that the performance gap between plain designs (ResNet-50|ViT-S/16) and advanced designs (ConvNeXt-T|Swin-T) no longer exists after applying ScaleKD. These phenomena indicate ScaleKD could have a potential impact on the model selection in real applications.

4 Ablation Study

4.1 Tightly Coupled Design Properties of Three Core Components

Recall that our ScaleKD consists of three core components, CAP, DFM and TPP, which are progressively designed in a tightly coupled manner. In Table 9a, we perform an ablation study to testify their complementarity via comparing different component combinations. We can notice: i) when gradually applying more of three component designs, the performance of ResNet-50 and Mixer-S shows similar increasing trends, showing that each component of ScaleKD is not designed for specific student architecture; ii) although CAP brings the two students promising performance gains, DFM and TPP further brings ResNet-50|Mixer-S extra performance gains, 0.64%|0.75% and 1.25%|1.39% respectively, verifying that DFM and TPP are complementary to CAP; iii) when using DFM and TPP together, both ResNet-50 and Mixer-S obtain additional performance boosts, which indicates that DFM and TPP are also complementary with each other.

4.2 Role of Each of Three Core Components

CAP vs. Popular Feature Projectors. We first compare CAP with two popular feature projectors, denoted as *Linear* and *Conv*, to verify the superiority of CAP. The former projector consists of a linear layer and the latter projector consists of two 3×3 convolutional layers. From the results shown in Table 9b, we can notice that CAP outperforms the other two projectors clearly, which validates the key role of CAP: aligning computing paradigm differences towards better KD performance.

Importance of Alternative Feature Mimicking in DFM. The key insight of DFM is to complement the neglected alternative features in the feature mimicking process. In Table 9c, we compare DFM with CAP and dual-path CAP to illustrate that the alternative feature mimicking is essential. We find that although the dual-path feature mimicking brings 0.25% extra performance gain to CAP, removing

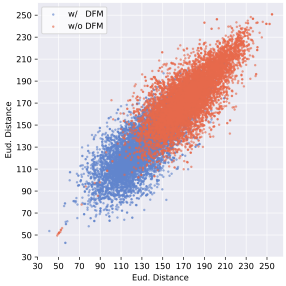

Figure 3: Feature distances of alternative components in the spatial domain. Details on the figure drawing are in Figure 6.

https://doi.org/10.52202/079017-2022

the direct component in the second path can further bring 0.39% improvement. This verifies the rationality of the design. To better understand why the performance gain is from the learning of teacher's alternative features, we make comparisons between the methods with DFM and without DFM. Specifically, we measure the distances between the student's features and the teacher's features of alternative components in the spatial domain. In Figure 3, we can clearly see that DFM can effectively reduce alternative feature distance between the teacher and the student.

Role of Proxy Path in TPP. Note that for transferring the teacher's pre-training knowledge in the parameter space to the student, TPP establishes a proxy path that connects the student's former stages to the teacher's later stages. In Table 9d, we study the design of TPP and verify whether the proxy path and its adaptive queries are effective. The results show that the feature mimicking in the proxy path can provide the student with performance improvement and providing input-dependent queries can further enhance the effectiveness of TPP, which indicates that these designs in TPP are essential for learning the knowledge in the teacher's parameter space.

More ablation studies on the hyper-parameter β and the others are provided in Appendix D.

5 Related Work

Knowledge Distillation. Traditional KD methods [14–35] generally focus on CNN-based teacher-student network pairs with small model scale gaps. Some recent works [54, 55, 50] further study how to conduct knowledge distillation with larger teachers. As vision transformers suffer from low convergence speeds, some recent works [56–58] explore leveraging CNNs to accelerate the training of vision transformers. Meanwhile, [36–38, 59] discuss how to bridge the architecture gap when the teacher and the student are in different model categories.

Frequency-based Knowledge Distillation. As traditional feature distillation only focuses on pixel-to-pixel differences, FAM [60] defines knowlwedge distillation in terms of frequency-based attention maps. FreeKD [61] explores how to eliminate unfavorable information in the frequency domain for enhancing the distillation performance on dense prediction tasks. Different from our ScaleKD, they consider feature distillation on CNN-based network pairs and have different formulations.

Teacher Parameter Reuse. Some previous KD methods also leverage the teacher's parameter for reusing a better classifier [32] or initializing the student's neck and head [62–64] or dismissing the shortcuts in residual architectures [65]. Unlike our ScaleKD, the motivation of these works focuses on parameter reuse or equivalent substitution, rather than aligning two parameter spaces for transferring the teacher's pre-training knowledge to the target student without the pre-training process.

6 Conclusion

In this paper, we present ScaleKD, a new cross architecture KD approach for transferring the scalable properties of pre-trained large ViTs to various CNNs, MLPs and heterogeneous ViTs. Our method consists of three tightly coupled components that rely on principled designs to align computing paradigm differences, model scale differences, and knowledge density differences between the teacher and the student. By conducting systematic experiments on several mainstream large-scale vision benchmarks, we broadly validate the effectiveness and generalization ability of our method. Benefiting from its novel motivation and design insights, ScaleKD is the first work which successfully verified that KD can be a more efficient alternative to the time-intensive pre-training, to the best of our knowledge. This extends the application scope of KD from model compression to training acceleration. We hope our work would inspire feature KD research in this new direction.

Limitations. Restricted by our computational resources, we do not conduct experiments on very large teachers, such as ViT-22B [66], or on large students, such as ViT-L [4]. Furthermore, with the increasing model scale of teachers, the training cost of ScaleKD increases, which is a common limitation to KD research. According to the analysis in Appendix D, the extra training cost of ScaleKD is acceptable to a large extent. Actually, thanks to its promising performance, ScaleKD shows the great potential to replace the time-intensive pre-training of students on large-scale datasets.

References

[1] Alex Krizhevsky, Ilya Sutskever, and Geoffrey E Hinton. Imagenet classification with deep convolutional neural networks. In *NIPS*, 2012.

[2] Kaiming He, Xiangyu Zhang, Shaoqing Ren, and Jian Sun. Deep residual learning for image recognition. In *CVPR*, 2016.

[3] Zhuang Liu, Hanzi Mao, Chao-Yuan Wu, Christoph Feichtenhofer, Trevor Darrell, and Saining Xie. A convnet for the 2020s. In *CVPR*, 2022.

[4] Alexey Dosovitskiy, Lucas Beyer, Alexander Kolesnikov, Dirk Weissenborn, Xiaohua Zhai, Thomas Unterthiner, Mostafa Dehghani, Matthias Minderer, Georg Heigold, Sylvain Gelly, et al. An image is worth 16x16 words: Transformers for image recognition at scale. In *ICLR*, 2020.

[5] Ze Liu, Yutong Lin, Yue Cao, Han Hu, Yixuan Wei, Zheng Zhang, Stephen Lin, and Baining Guo. Swin transformer: Hierarchical vision transformer using shifted windows. In *ICCV*, 2021.

[6] Ilya O Tolstikhin, Neil Houlsby, Alexander Kolesnikov, Lucas Beyer, Xiaohua Zhai, Thomas Unterthiner, Jessica Yung, Andreas Steiner, Daniel Keysers, Jakob Uszkoreit, et al. Mlp-mixer: An all-mlp architecture for vision. In *NeurIPS*, 2021.

[7] Hugo Touvron, Piotr Bojanowski, Mathilde Caron, Matthieu Cord, Alaaeldin El-Nouby, Edouard Grave, Gautier Izacard, Armand Joulin, Gabriel Synnaeve, Jakob Verbeek, et al. Resmlp: Feedforward networks for image classification with data-efficient training. *TPAMI*, 2022.

[8] Hanxiao Liu, Zihang Dai, David So, and Quoc V Le. Pay attention to mlps. In *NeurIPS*, 2021.

[9] Ashish Vaswani, Noam Shazeer, Niki Parmar, Jakob Uszkoreit, Llion Jones, Aidan N Gomez, Łukasz Kaiser, and Illia Polosukhin. Attention is all you need. In *NIPS*, 2017.

[10] Kaiming He, Xinlei Chen, Saining Xie, Yanghao Li, Piotr Dollár, and Ross Girshick. Masked autoencoders are scalable vision learners. In *CVPR*, 2022.

[11] Jinghao Zhou, Chen Wei, Huiyu Wang, Wei Shen, Cihang Xie, Alan Yuille, and Tao Kong. Image bert pre-training with online tokenizer. In *ICLR*, 2021.

[12] Alec Radford, Jong Wook Kim, Chris Hallacy, Aditya Ramesh, Gabriel Goh, Sandhini Agarwal, Girish Sastry, Amanda Askell, Pamela Mishkin, Jack Clark, et al. Learning transferable visual models from natural language supervision. In *ICML*, 2021.

[13] Mehdi Cherti, Romain Beaumont, Ross Wightman, Mitchell Wortsman, Gabriel Ilharco, Cade Gordon, Christoph Schuhmann, Ludwig Schmidt, and Jenia Jitsev. Reproducible scaling laws for contrastive language-image learning. In *CVPR*, 2023.

[14] Geoffrey Hinton, Oriol Vinyals, and Jeff Dean. Distilling the knowledge in a neural network. *arXiv preprint arXiv:1503.02531*, 2015.

[15] Adriana Romero, Nicolas Ballas, Samira Ebrahimi Kahou, Antoine Chassang, Carlo Gatta, and Yoshua Bengio. Fitnets: Hints for thin deep nets. In *ICLR*, 2015.

[16] Sergey Zagoruyko and Nikos Komodakis. Paying more attention to attention: Improving the performance of convolutional neural networks via attention transfer. In *ICLR*, 2016.

[17] Sungsoo Ahn, Shell Xu Hu, Andreas Damianou, Neil D Lawrence, and Zhenwen Dai. Variational information distillation for knowledge transfer. In *CVPR*, 2019.

[18] Frederick Tung and Greg Mori. Similarity-preserving knowledge distillation. In *ICCV*, 2019.

[19] Baoyun Peng, Xiao Jin, Jiaheng Liu, Dongsheng Li, Yichao Wu, Yu Liu, Shunfeng Zhou, and Zhaoning Zhang. Correlation congruence for knowledge distillation. In *ICCV*, 2019.

[20] Wonpyo Park, Dongju Kim, Yan Lu, and Minsu Cho. Relational knowledge distillation. In *CVPR*, 2019.

 https://doi.org/10.52202/079017-2022

[21] Nikolaos Passalis and Anastasios Tefas. Learning deep representations with probabilistic knowledge transfer. In *ECCV*, 2018.

[22] Byeongho Heo, Minsik Lee, Sangdoo Yun, and Jin Young Choi. Knowledge transfer via distillation of activation boundaries formed by hidden neurons. In *AAAI*, 2019.

[23] Jangho Kim, SeongUk Park, and Nojun Kwak. Paraphrasing complex network: Network compression via factor transfer. In *NeurIPS*, 2018.

[24] Junho Yim, Donggyu Joo, Jihoon Bae, and Junmo Kim. A gift from knowledge distillation: Fast optimization, network minimization and transfer learning. In *CVPR*, 2017.

[25] Yonglong Tian, Dilip Krishnan, and Phillip Isola. Contrastive representation distillation. In *ICLR*, 2020.

[26] Byeongho Heo, Jeesoo Kim, Sangdoo Yun, Hyojin Park, Nojun Kwak, and Jin Young Choi. A comprehensive overhaul of feature distillation. In *ICCV*, 2019.

[27] Guodong Xu, Ziwei Liu, Xiaoxiao Li, and Chen Change Loy. Knowledge distillation meets self-supervision. In *ECCV*, 2020.

[28] Xiatian Zhu, Shaogang Gong, et al. Knowledge distillation by on-the-fly native ensemble. In *NeurIPS*, 2018.

[29] Guile Wu and Shaogang Gong. Peer collaborative learning for online knowledge distillation. In *AAAI*, 2021.

[30] Jing Yang, Brais Marinez, Bulat Adrian, and Tzimiropoulos Georgios. Knowledge distillation via softmax regression representation learning. In *ICLR*, 2021.

[31] Defang Chen, Jian-Ping Mei, Yuan Zhang, Can Wang, Zhe Wang, Yan Feng, and Chun Chen. Cross-layer distillation with semantic calibration. In *AAAI*, 2021.

[32] Defang Chen, Jian-Ping Mei, Hailin Zhang, Can Wang, Yan Feng, and Chun Chen. Knowledge distillation with the reused teacher classifier. In *CVPR*, 2022.

[33] Xueqing Deng, Dawei Sun, Shawn Newsam, and Peng Wang. Distpro: Searching a fast knowledge distillation process via meta optimization. In *ECCV*, 2022.

[34] Xiaolong Liu, Lujun Li, Chao Li, and Anbang Yao. Norm: Knowledge distillation via n-to-one representation matching. In *ICLR*, 2023.

[35] Borui Zhao, Quan Cui, Renjie Song, Yiyu Qiu, and Jiajun Liang. Decoupled knowledge distillation. In *CVPR*, 2022.

[36] Zhiwei Hao, Jianyuan Guo, Kai Han, Yehui Tang, Han Hu, Yunhe Wang, and Chang Xu. One-for-all: Bridge the gap between heterogeneous architectures in knowledge distillation. In *NeurIPS*, 2023.

[37] Yufan Liu, Jiajiong Cao, Bing Li, Weiming Hu, Jingting Ding, and Liang Li. Cross-architecture knowledge distillation. In *ACCV*, 2022.

[38] Yixuan Wei, Han Hu, Zhenda Xie, Zheng Zhang, Yue Cao, Jianmin Bao, Dong Chen, and Baining Guo. Contrastive learning rivals masked image modeling in fine-tuning via feature distillation. *arXiv preprint arXiv:2205.14141*, 2022.

[39] Zhendong Yang, Zhe Li, Ailing Zeng, Zexian Li, Chun Yuan, and Yu Li. Vitkd: Feature-based knowledge distillation for vision transformers. In *CVPRW*, 2024.

[40] Hangbo Bao, Li Dong, Songhao Piao, and Furu Wei. Beit: Bert pre-training of image transformers. In *ICLR*, 2021.

[41] Yuxin Fang, Wen Wang, Binhui Xie, Quan Sun, Ledell Wu, Xinggang Wang, Tiejun Huang, Xinlong Wang, and Yue Cao. Eva: Exploring the limits of masked visual representation learning at scale. In *CVPR*, 2023.

[42] Lvmin Zhang, Anyi Rao, and Maneesh Agrawala. Adding conditional control to text-to-image diffusion models. In *ICCV*, 2023.

[43] Alexander Kirillov, Eric Mintun, Nikhila Ravi, Hanzi Mao, Chloe Rolland, Laura Gustafson, Tete Xiao, Spencer Whitehead, Alexander C Berg, Wan-Yen Lo, et al. Segment anything. In *CVPR*, 2023.

[44] Robin Rombach, Andreas Blattmann, Dominik Lorenz, Patrick Esser, and Björn Ommer. High-resolution image synthesis with latent diffusion models. In *CVPR*, 2022.

[45] Jia Deng, Wei Dong, Richard Socher, Li-Jia Li, Kai Li, and Li Fei-Fei. Imagenet: A large-scale hierarchical image database. In *CVPR*, 2009.

[46] Tsung-Yi Lin, Michael Maire, Serge Belongie, James Hays, Pietro Perona, Deva Ramanan, Piotr Dollár, and C Lawrence Zitnick. Microsoft coco: Common objects in context. In *ECCV*, 2014.

[47] Bolei Zhou, Hang Zhao, Xavier Puig, Tete Xiao, Sanja Fidler, Adela Barriuso, and Antonio Torralba. Semantic understanding of scenes through the ade20k dataset. *IJCV*, 2019.

[48] Christoph Schuhmann, Romain Beaumont, Richard Vencu, Cade Gordon, Ross Wightman, Mehdi Cherti, Theo Coombes, Aarush Katta, Clayton Mullis, Mitchell Wortsman, et al. Laion-5b: An open large-scale dataset for training next generation image-text models. *NeurIPS*, 2022.

[49] Yuxin Fang, Quan Sun, Xinggang Wang, Tiejun Huang, Xinlong Wang, and Yue Cao. Eva-02: A visual representation for neon genesis. *arXiv preprint arXiv:2303.11331*, 2023.

[50] Tao Huang, Shan You, Fei Wang, Chen Qian, and Chang Xu. Knowledge distillation from a stronger teacher. In *NeurIPS*, 2022.

[51] Tao Huang, Yuan Zhang, Mingkai Zheng, Shan You, Fei Wang, Chen Qian, and Chang Xu. Knowledge diffusion for distillation. In *NeurIPS*, 2023.

[52] Lucas Beyer, Xiaohua Zhai, Amélie Royer, Larisa Markeeva, Rohan Anil, and Alexander Kolesnikov. Knowledge distillation: A good teacher is patient and consistent. In *CVPR*, 2022.

[53] Ao Wang, Hui Chen, Zijia Lin, Hengjun Pu, and Guiguang Ding. Repvit: Revisiting mobile cnn from vit perspective. *arXiv preprint arXiv:2307.09283*, 2023.

[54] Seyed Iman Mirzadeh, Mehrdad Farajtabar, Ang Li, Nir Levine, Akihiro Matsukawa, and Hassan Ghasemzadeh. Improved knowledge distillation via teacher assistant. In *AAAI*, 2020.

[55] Wonchul Son, Jaemin Na, Junyong Choi, and Wonjun Hwang. Densely guided knowledge distillation using multiple teacher assistants. In *ICCV*, 2021.

[56] Hugo Touvron, Matthieu Cord, Matthijs Douze, Francisco Massa, Alexandre Sablayrolles, and Hervé Jégou. Training data-efficient image transformers & distillation through attention. In *International conference on machine learning*, 2021.

[57] Xianing Chen, Qiong Cao, Yujie Zhong, Jing Zhang, Shenghua Gao, and Dacheng Tao. Dearkd: Data-efficient early knowledge distillation for vision transformers. In *CVPR*, 2022.

[58] Borui Zhao, Renjie Song, and Jiajun Liang. Cumulative spatial knowledge distillation for vision transformers. In *ICCV*, 2023.

[59] Jinjing Zhu, Yunhao Luo, Xu Zheng, Hao Wang, and Lin Wang. A good student is cooperative and reliable: Cnn-transformer collaborative learning for semantic segmentation. In *ICCV*, 2023.

[60] Cuong Pham, Van-Anh Nguyen, Trung Le, Dinh Phung, Gustavo Carneiro, and Thanh-Toan Do. Frequency attention for knowledge distillation. In *WACV*, 2024.

[61] Yuan Zhang, Tao Huang, Jiaming Liu, Tao Jiang, Kuan Cheng, and Shanghang Zhang. Freekd: Knowledge distillation via semantic frequency prompt. In *CVPR*, 2024.

 https://doi.org/10.52202/079017-2022

[62] Zijian Kang, Peizhen Zhang, Xiangyu Zhang, Jian Sun, and Nanning Zheng. Instance-conditional knowledge distillation for object detection. In *NeurIPS*, 2021.

[63] Zhendong Yang, Zhe Li, Xiaohu Jiang, Yuan Gong, Zehuan Yuan, Danpei Zhao, and Chun Yuan. Focal and global knowledge distillation for detectors. In *CVPR*, 2022.

[64] Jiabao Wang, Yuming Chen, Zhaohui Zheng, Xiang Li, Ming-Ming Cheng, and Qibin Hou. Crosskd: Cross-head knowledge distillation for object detection. In *CVPR*, 2024.

[65] Guilin Li, Junlei Zhang, Yunhe Wang, Chuanjian Liu, Matthias Tan, Yunfeng Lin, Wei Zhang, Jiashi Feng, and Tong Zhang. Residual distillation: Towards portable deep neural networks without shortcuts. In *NeurIPS*, 2020.

[66] Mostafa Dehghani, Josip Djolonga, Basil Mustafa, Piotr Padlewski, Jonathan Heek, Justin Gilmer, Andreas Peter Steiner, Mathilde Caron, Robert Geirhos, Ibrahim Alabdulmohsin, et al. Scaling vision transformers to 22 billion parameters. In *ICML*, 2023.

[67] MMPreTrain Contributors. Openmmlab's pre-training toolbox and benchmark. `https://github.com/open-mmlab/mmpretrain`, 2023.

[68] Andrew G Howard, Menglong Zhu, Bo Chen, Dmitry Kalenichenko, Weijun Wang, Tobias Weyand, Marco Andreetto, and Hartwig Adam. Mobilenets: Efficient convolutional neural networks for mobile vision applications. *arXiv preprint arXiv:1704.04861*, 2017.

[69] Pengguang Chen, Shu Liu, Hengshuang Zhao, and Jiaya Jia. Distilling knowledge via knowledge review. In *CVPR*, 2021.

[70] Zhendong Yang, Zhe Li, Mingqi Shao, Dachuan Shi, Zehuan Yuan, and Chun Yuan. Masked generative distillation. In *ECCV*, 2022.

[71] Kai Chen, Jiaqi Wang, Jiangmiao Pang, Yuhang Cao, Yu Xiong, Xiaoxiao Li, Shuyang Sun, Wansen Feng, Ziwei Liu, Jiarui Xu, Zheng Zhang, Dazhi Cheng, Chenchen Zhu, Tianheng Cheng, Qijie Zhao, Buyu Li, Xin Lu, Rui Zhu, Yue Wu, Jifeng Dai, Jingdong Wang, Jianping Shi, Wanli Ouyang, Chen Change Loy, and Dahua Lin. MMDetection: Open mmlab detection toolbox and benchmark. *arXiv preprint arXiv:1906.07155*, 2019.

[72] MMSegmentation Contributors. MMSegmentation: Openmmlab semantic segmentation toolbox and benchmark. `https://github.com/open-mmlab/mmsegmentation`, 2020.

[73] Kaiming He, Georgia Gkioxari, Piotr Dollár, and Ross Girshick. Mask r-cnn. In *ICCV*, 2017.

[74] Tete Xiao, Yingcheng Liu, Bolei Zhou, Yuning Jiang, and Jian Sun. Unified perceptual parsing for scene understanding. In *ECCV*, 2018.

[75] Alex Krizhevsky, Geoffrey Hinton, et al. Learning multiple layers of features from tiny images. *Tech Report*, 2009.

[76] Xiaohan Ding, Yiyuan Zhang, Yixiao Ge, Sijie Zhao, Lin Song, Xiangyu Yue, and Ying Shan. Unireplknet: A universal perception large-kernel convnet for audio, video, point cloud, time-series and image recognition. *arXiv preprint arXiv:2311.15599*, 2023.

[77] Mingxing Tan and Quoc Le. Efficientnet: Rethinking model scaling for convolutional neural networks. In *ICML*, 2019.

[78] Kan Wu, Jinnian Zhang, Houwen Peng, Mengchen Liu, Bin Xiao, Jianlong Fu, and Lu Yuan. Tinyvit: Fast pretraining distillation for small vision transformers. In *ECCV*, 2022.

[79] Li Yuan, Yunpeng Chen, Tao Wang, Weihao Yu, Yujun Shi, Zi-Hang Jiang, Francis EH Tay, Jiashi Feng, and Shuicheng Yan. Tokens-to-token vit: Training vision transformers from scratch on imagenet. In *ICCV*, 2021.

[80] Mingyu Ding, Bin Xiao, Noel Codella, Ping Luo, Jingdong Wang, and Lu Yuan. Davit: Dual attention vision transformers. In *ECCV*, 2022.

[81] Jiahao Wang, Wenqi Shao, Mengzhao Chen, Chengyue Wu, Yong Liu, Kaipeng Zhang, Songyang Zhang, Kai Chen, and Ping Luo. Adapting llama decoder to vision transformer. *arXiv preprint arXiv:2404.06773*, 2024.

Appendix for "ScaleKD: Strong Vision Transformers Could Be Excellent Teachers"

Jiawei Fan[*]
Intel Labs China
jiawei.fan@intel.com

Chao Li[*]
Intel Labs China
chao3.li@intel.com

Xiaolong Liu[*]
iMotion Automotive Technology
xiaolong.liu@imotion.ai

Anbang Yao[*†]
Intel Labs China
anbang.yao@intel.com

A Datasets

ImageNet-1K [45] is a well-known large-scale classification dataset, comprising over 1.2 million training images and 50,000 validation images with 1,000 object categories.

MS-COCO [46] is a large-scale dataset for object detection and instance segmentation, which contains 118,000 training images and 5,000 validation images with 80 object categories.

ADE20K [47] is a challenging semantic segmentation dataset, containing 20,210 training samples, 2,000 validation samples, and 3,352 testing samples with 150 categories.

B Experimental Setups

B.1 Experimental Setups on IN-1K

Training Strategy. We conduct our experiments with two popular training strategies: traditional training strategy and advanced training strategy. The traditional training strategy is commonly used in previous KD approaches (shown in Table 10a) and the advanced training strategy is adopted in training recently proposed CNNs, MLPs, and ViTs (shown in Table 10b).

Compute Infrastructure. The experiments using the traditional training strategy are conducted on 8 $\times$ NVIDIA Tesla-V100 GPUs, while the experiments using the advanced training strategy are conducted on 32 $\times$ NVIDIA Tesla-V100 GPUs.

Implementation Codebase. We implement our method based on MMClassification [67].

Hyper-Parameter Settings. The overall loss for our ScaleKD is defined as Equation 5. Thanks to the simplicity of this formulation, we have only one hyper-parameter β in our ScaleKD. From the ablation study in the Appendix D, we find that the best choice is $\beta = 0.6$ and we use it as the default setting throughout all experiments.

Selection of Teacher-Student Network Pairs. Overall, we construct 11 teacher-student network pairs, which consist of 2 pre-trained large ViTs, and 10 students covering mainstream architectures of ViT, MLP, and CNN. Specifically, for the teacher, we choose two different types of well pre-trained ViTs: supervised pre-trained Swin-L [5] with the hierarchical architecture and hybrid pre-trained BEiT-L/14 [40] with the typical ViT architecture. Moreover, compared to Swin-L, BEiT-L/14 is much larger in terms of model size and stronger in terms of model performance. For the student

[*] Core authors contributed to method formulation, experimental design and analysis.
[†] Corresponding author.

38th Conference on Neural Information Processing Systems (NeurIPS 2024).

https://doi.org/10.52202/079017-2022

Table 10: Detailed settings of traditional training strategy and advanced training strategy on IN-1K.

(a) Traditional training strategy

Configuration	CNN
Batch Size	256
Learning Rate	0.1
Learning Rate Schedule	Stepwise Decay/Cosine Decay
Optimizer	SGD
Optimizer Hyper-Parameters	momentum= 0.9
Weight Decay	1e-4
Training Epochs	100
Warmup Epochs	✗
Drop Path	✗
Label Smoothing	✗
Random Flip	0.5
Random Resize Crop	(0.08,1)
Random Augmentation	✗
Random Erasing	✗

(b) Advanced training strategy

Configuration	CNN / MLP / ViT
Batch Size	2048 / 1536 / 1024
Learning Rate	5e-3 / 7e-4 / 1e-3
Learning Rate Schedule	Cosine Decay
Optimizer	Lamb / AdamW / AdamW
Optimizer Hyper-Parameters	$\beta_1, \beta_2, \epsilon = 0.9, 0.009$, 1e-8
Weight Decay	0.02 / 0.07 /0.05
Training Epochs	300
Warmup Epochs	5 / 20 / 20
Drop Path	0.05 / 0.1 / 0.1
Label Smoothing	0.1
Random Flip	0.5
Random Resize Crop	(0.08,1)
Random Augmentation	(7,0.5) / (9,0.5) / (9,0.5)
Random Erasing	0.25

Table 11: Detailed settings of transfer learning strategies on MS-COCO and ADE20K.

(a) MS-COCO

Configuration	ResNet-50 / Swin-S
Weight Initialization	Pre-trained Checkpoint
Batch Size	16
Learning Rate	1e-4
Learning Rate Decay	Stage (0.7)
Learning Rate Schedule	Cosine Decay
Optimizer	AdamW
Optimizer Hyper-Parameters	$\beta_1, \beta_2, \epsilon = 0.9, 0.009$, 1e-8
Weight Decay	0.05
Training Epochs	8
Crop Size	(1333, 800)
Drop Path	0.0 / 0.2

(b) ADE20K

Configuration	ResNet-50 / Swin-S / ViT-B
Weight Initialization	Pre-trained Checkpoint
Batch Size	16
Learning Rate Decay	1e-4 / 1e-4 / 2e-4
LR decay	Stage (0.9) / Stage (0.9) / Layer (0.6)
Learning Rate Schedule	Cosine Decay
Optimizer	AdamW
Optimizer Hyper-Parameters	$\beta_1, \beta_2, \epsilon = 0.9, 0.009$, 1e-8
Weight Decay	0.05
Training Iterations	160000
Crop Size	(512, 512)
Drop Path	0.0 / 0.3 / 0.2

architectures, we first choose the basic design in each architecture type, such as ResNet-50 [2], Mixer-S/16 [6], and ViT-S/16 [4]. Then, we also select some popular models, such as MobileNet-V1 [68], ConvNeXt-T [3], and Swin-S. Next, we expand the basic designs to larger ones, like Mixer-B/16, Mixer-B/14, ViT-B/16 and ViT-B/14. After separately selecting teachers and students, we finally organize them into 11 teacher-student network pairs for comprehensive experiments. Note that the performance for most individual trained baselines in Table 3 are sourced from their original papers, except for ResNet-50, MobileNet-V1, ViT-B/14, and Mixer-B/14, which we trained ourselves using the advanced training strategy due to the absence of reference results in their original papers.

Counterpart Pre-training Methods. In the main paper, we select state-of-the-art methods in each pre-training paradigm for comparison. For supervised pre-training, we choose the pioneering work [4]. For self-supervised pre-training, we choose BEiT [40] and iBoT [11]. For cross-modal pre-training and hybrid pre-training, we choose CLIP [13] and EVA-02 [49], respectively.

Counterpart Knowledge Distillation Methods. In the main paper, we make comparisons with many recent KD methods, such as DIST [50], DiffKD [51], OFA [36] and FuncMatch [52]. In this Appendix, we further compare with CNN-based methods, such as KD [14], AT [16], OFD [26], RKD [20], CRD [25], DKD [35], SRRL [30], ReviewKD [69], DistPro [33] and MGD [70].

Counterpart Model Engineering Methods. In the main paper, to better show the great potential of our ScaleKD, we apply it to the popular designs of each architecture type and make comparisons with various advanced counterparts. Driven by this target, we mainly select the so-called next-generation models. For ResNet-50, we select ConvNeXt-T [3] and RepViT-2.3M [53] for comparison. The former one is the typical design of the new-era CNN and the latter one is a popular model for deployment. For Mixer-B, we select gMLP-B [8] and ResMLP-B24 [7], which are optimized to

Table 12: Performance comparison (%) of ScaleKD and CLIP on ViT-B for linear probing.

Model	Method	Pre-training Dataset	IN-1K (Training)	CIFAR-100 (Linear Probing)				
				1 shot	5 shot	10 shot	25 shot	Full
ViT-B/16	From-scratch	IN-1K	81.80	33.86	60.30	66.77	72.65	81.76
	CLIP	LAION-300M	-	-	-	71.96	77.21	84.07
		LAION-2B, IN-1K	85.49	41.10	69.00	72.34	78.64	85.51
		LAION-2B, IN-12K, IN-1K	86.17	44.90	70.19	76.77	81.43	88.88
		CLIP OpenAI, IN-12K, IN-1K	85.99	47.40	70.85	77.37	**81.52**	88.92
ViT-B/14	Ours	IN-1K	86.43	**48.14**	**70.91**	**77.52**	81.50	**89.11**
Teacher: BEiT-L/14	EVA	CLIP OpenAI, IN-22K, IN-1K	88.58	63.74	85.20	87.39	89.27	93.36

Table 13: Performance comparison on IN-1K with more CNN-based KD methods. In the experiment, we adopt the same traditional training strategy as these methods.

Model	Teacher	Method	Top-1(%)
MobileNet-V1	ResNet-50 (76.16)	From Scratch	69.63
		KD [14]	70.68
		AT [16]	70.72
		OFD [26]	71.25
		RKD [20]	71.23
		CRD [25]	71.40
		DKD [35]	72.05
		SRRL [30]	72.49
		ReviewKD [69]	72.56
		DIST [50]	73.24
		DistPro [33]	73.26
		MGD [70]	73.35
		DiffKD [51]	73.62
	Swin-L (86.24)	ScaleKD	**74.21**

suppress the weaknesses of MLP-Mixer. For ViT-S, we choose Swin-S [5] and Swin-B as counterparts to validate whether our ScaleKD could outperform larger advanced designs.

B.2 Experimental Setups on MS-COCO and ADE20K

Training Strategy and Hyper-Parameter Settings. For the experiments on MS-COCO, we adopt the settings shown in Table 11a, while for experiments on ADE20K, we adopt the settings shown in Table 11b.

Compute Infrastructure. All experiments on MS-COCO and ADE20K are conducted on 8 $\times$ NVIDIA Tesla-V100 GPUs.

Implementation Codebase. We conduct experiments based on MMDetection [71] and MMSegmentation [72].

Selection of Task Frameworks and Backbones. For different task frameworks, we choose Mask R-CNN [73] for object detection and instance segmentation, and UperNet [74] for semantic segmentation. As for backbones, we select ResNet-50, Swin-T, and ViT-B/16.

C More Experiments

Linear Probing on CIFAR-100. We conduct a set of linear probing experiments on CIFAR-100 [75], based on models in Table 4. From the results shown in Table 12, we can observe: i) models pre-trained by CLIP greatly improve the backbone's generalization ability across different datasets; ii) our ScaleKD helps the student model reach mostly better performance than CLIP-based pre-training, even without viewing pre-training data.

Performance Comparison with More KD Methods. In the main paper, we compare ScaleKD with mostly related cross architecture KD approaches in Table 7, as few previous works use medium-sized students, such as ResNet-50, for benchmarking. To make a more comprehensive comparison with lots of CNN-based KD methods, we conduct experiments on a traditional student network, MobileNet-V1,

https://doi.org/10.52202/079017-2022

Table 14: Performance comparison on IN-1K with lots of model engineering methods. We conduct ScaleKD on the simplest design of each architecture type and then make a performance comparison with various designs. Ours*, Ours† and Ours‡ denote choosing ViT-B (training from scratch), Swin-L (with IN-22K pre-training) and BEiT-L/14 (with EVA pre-training) as the teacher, respectively.

Model	Training Dataset	Resolution	Params (M)	FLOPs (G)	Top-1(%)
CNN-based Architecture					
ConvNext-T [3]	IN-1K	224^2	28.59	4.46	82.14
ConvNext-T + Ours†	IN-1K	224^2	28.59	4.46	84.16
ConvNext-T [3]	IN-22K $\Rightarrow$ IN-1K	224^2	28.59	4.46	82.90
ConvNext-B [3]	IN-1K	224^2	87.77	15.14	83.80
UniRepLKNet-T [76]	IN-1K	224^2	31.00	4.90	83.20
EfficientNet-B5 [77]	IN-1K	456^2	30.00	9.90	83.60
RepViT-M2.3 [53]	IN-1K	224^2	22.90	-	83.70
MLP-based Architecture					
Mixer-B/16 [6]	IN-1K	224^2	59.88	12.61	76.44
Mixer-B/16 + Ours*	IN-1K	224^2	59.88	12.61	81.62
Mixer-B/16 + Ours†	IN-1K	224^2	59.88	12.61	81.96
Mixer-B/14 + Ours‡	IN-1K	224^2	59.88	16.45	82.89
Mixer-B/16 [6]	IN-22K $\Rightarrow$ IN-1K	224^2	59.88	12.61	80.64
Mixer-L/16 [6]	IN-22K $\Rightarrow$ IN-1K	224^2	208.2	44.57	82.89
ResMLP-B24 [7]	IN-1K	224^2	115.7	23.0	81.00
gMLP-B [8]	IN-1K	224^2	73.00	15.80	81.60
Transformer-based Architecture					
ViT-S/16 [4]	IN-1K	224^2	22.05	4.61	79.90
ViT-S/16 + Ours†	IN-1K	224^2	22.05	4.61	83.93
ViT-S/16 [4, 78]	IN-22K $\Rightarrow$ IN-1K	224^2	22.05	4.61	80.50
Swin-T [5, 78]	IN-22K $\Rightarrow$ IN-1K	224^2	28.29	4.36	81.90
T2T-ViT$_t$-14 [79]	IN-1K	224^2	21.47	4.34	81.83
DaViT-T [80]	IN-1K	224^2	28.36	4.54	82.24
iLLaMA-S [81]	IN-1K	224^2	21.90	-	79.90
EVA-02-S/14 [49]	IN-1K	336^2	22.13	15.51	81.12
EVA-02-S/14 + Ours‡	IN-1K	336^2	22.13	15.51	86.22
ViT-B/16 [4]	IN-1K	224^2	86.57	17.58	81.80
Swin-B [5]	IN-1K	224^2	87.77	15.14	83.50
T2T-ViT$_t$-24 [79]	IN-1K	224^2	64.00	12.69	82.71
DaViT-B [80]	IN-1K	224^2	87.95	15.51	84.09
ViT-B/16 [4]	IN-22K $\Rightarrow$ IN-1K	224^2	86.57	17.58	83.97
Swin-B [5]	IN-22K $\Rightarrow$ IN-1K	224^2	87.77	15.14	85.20
iLLaMA-B [81]	IN-22K $\Rightarrow$ IN-1K	224^2	86.30	-	85.00

using the same training strategy as them. From the results shown in Table 13, we can observe that by using Swin-L as the teacher, our ScaleKD could help MobileNet-V1 reach 74.21% top-1 accuracy, outperforming previous methods which use ResNet-50 as the teacher by clear margins.

Performance Comparison with More Model Engineering Methods. In the main paper, we apply ScaleKD to the basic design of each architecture type and make comparisons with more recent variant architectures. As illustrated in Table 14, we choose more designs to have a more comprehensive comparison.

D More Ablation Studies

Ablation Study on Training Efficiency of ScaleKD. As TPP in our ScaleKD leverages the teacher's last stage, it will introduce additional training costs compared to traditional FD. To clearly study its training efficiency, we conduct ablative experiments in this section: i) as shown in Table 15a, we first compare the training efficiency of ScaleKD with traditional FD on three network pairs having increased teacher's model scale; ii) then, as shown in Table 15b, we conduct the experiments on each component in ScaleKD. The experimental results show that: i) using large teachers would

Table 15: Experiments on the training efficiency of ScaleKD. The student model in all experiments is ResNet-50. In (a), we compare ScaleKD with traditional FD using three teachers with different model scales. In (b), we conduct the experiments based on Swin-S→ResNet-50 teacher-student network pair to illustrate the training costs (memory and time) introduced by each component of ScaleKD. Experiments are conducted on 8 × NVIDIA Tesla-V100 GPUs.

(a) Training costs comparison with FD

Teacher	Method	Top-1 (%)	GPU Memory (G)	T_{train} (d)
Swin-S	FD	77.43	3.66	1.67
	ScaleKD	79.62	6.65	2.10
Swin-B	FD	77.76	3.66	1.83
	ScaleKD	79.80	7.26	2.53
Swin-L	FD	77.72	4.72	2.24
	ScaleKD	80.10	9.11	3.51

(b) Training costs of each component in ScaleKD

Method	Designs				Top-1 (%)	GPU Memory (G)	T_{train} (d)
	CAP	DFM	TPP	KD			
FD	-	-	-	-	77.43	3.66	1.67
ScaleKD	✓				77.87	3.77	1.70
	✓	✓			78.51	4.02	1.77
	✓		✓		78.62	5.13	1.84
	✓	✓	✓		79.30	6.60	2.08
	✓	✓	✓	✓	79.62	6.65	2.10

Table 16: Ablation study on pre-training and distillation.

Model	Method	Top-1(%)
ViT-S/16	Training from scratch on IN-1K	79.90
	Training from scratch on IN-1K w/ KD	81.42
	Pre-training on IN-22K	80.05
	Pre-training on IN-22K w/ KD	82.00
	Training from scratch on IN-1K w/ ScaleKD	83.93

Table 17: Ablation study on the necessity of alternative components in the first path of DFM.

Method	Top-1 (%)	Δ Top-1 (%)
Baseline	76.55	-
CAP	77.87	+1.32
DFM (Dir + Alt)	78.23	+1.68
DFM (All + Alt)	78.51	+1.96

induce more GPU memory occupation and longer training time; ii) comparatively, TPP is the most resource-consuming component, especially after combining it with DFM. In summary, our ScaleKD introduces additional training costs compared to traditional FD. However, if considering the significant performance gain it brings, these additional costs are acceptable.

Ablation Study on Hyper-parameter β. According to Equation 5 in the main paper, our method only has one hyper-parameter β, which is the balancing weight of two feature mimicking paths in DFM. We conduct the ablation study on Swin-S→ResNet-50 network pair to study the impact of different settings of β. Specifically, we select the β uniformly from 0 to 1. $\beta = 1.0$ indicates that only the first feature mimicking path exists, while $\beta = 0$ indicates that only the second feature mimicking path exists. As shown in Figure 4, we can observe: i) in general, ScaleKD outperforms the baseline by significant margins at all settings, validating the stability of ScaleKD; ii) when $\beta = 0.6$, our ScaleKD achieves the best performance; iii) though the second feature mimicking path could be used individually, it is inferior to the first path, indicating that the direct component is essential in feature mimicking; iv) when the two paths work collaboratively, they perform better than two individual counterparts, which suggests that the two designs are complementary with each other.

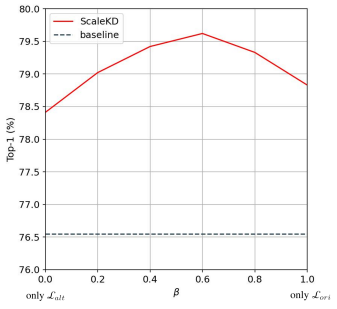

Figure 4: Ablation study on the hyper-parameter β.

Ablation Study on Pre-training and Distillation. In this study, we explore the originality of the distillation performance gain. We compare models trained by ScaleKD with upstream pre-trained models and upstream pre-training models with KD. From the results shown in Table 16, we can notice: i) compared to individual pre-training, applying KD under this stage can significantly boost model performance; ii) ViT-S/16 trained by ScaleKD significantly outperforms the models trained with KD on IN-22K. These two observations indicate that: i) small students are difficult to capture the pre-training knowledge with traditional FD, even with the upstream pre-training dataset; ii) our ScaleKD could effectively help the student to learn useful pre-training knowledge from the teacher without viewing the pre-training dataset.

Ablation Study on the First Feature Mimicking Path of DFM. We explore the necessity of alternative components in the first feature mimicking path of DFM. Specifically, we remove all alternative components in the first path of DFM and perform an experiment under the same settings as Table 9(b). For the results shown in Table 17, DFM(Dir + Alt) indicates the above new setting, while DFM(All+ Alt) is the original design. We can observe that removing all alternative components in the

https://doi.org/10.52202/079017-2022

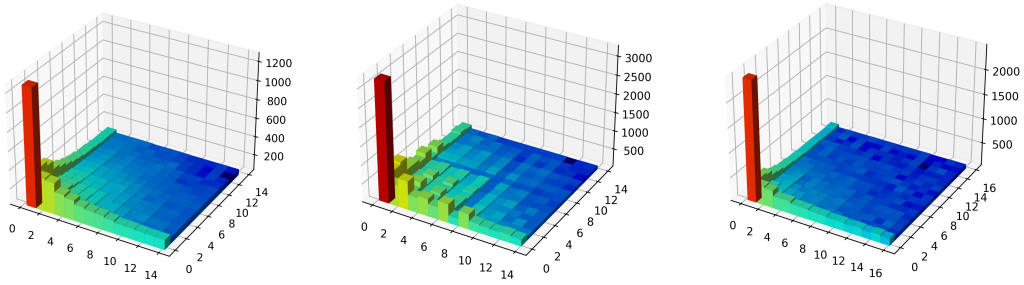

(a) ViT-L/14 (b) Swin-L (c) BEiT-L/14

Figure 5: More illustrative feature distributions of large pre-trained ViTs in the frequency domain. We first collect the output feature maps of 1600 samples from IN-1K, then conduct DCT on each channel, and finally take the average value across these samples after converting all responses into absolute values.

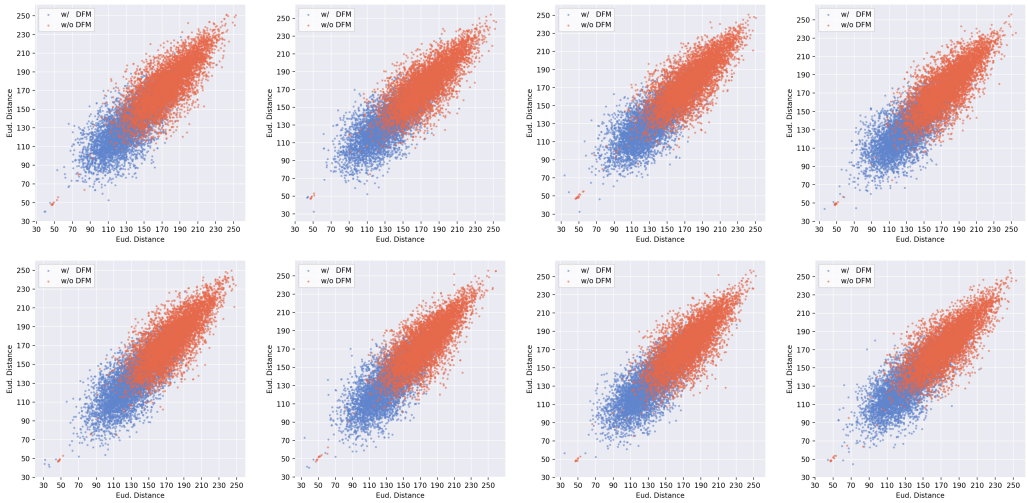

Figure 6: Feature distance distributions of alternative components for the last stage features between teacher and student on IN-1K. We obtain 64,000 feature pairs on Swin-L→ResNet-50 network pair from 64,000 samples. After calculating the distance between teacher and student, we project the high-dimension distances into a two-dimension space for illustration. Finally, we randomly select 6,400 data points for 8 times to draw the scatters. Blue points denote the distances without DFM, while orange points denote the distances with DFM.

first path will slightly decrease the effectiveness of DFM, but its performance is still obviously higher than CAP. As we discussed in Section 1, the first path of DFM aims to capture the teacher's global features, where the subtle alternative components are also indispensable parts. Directly removing alternative components in the first path will break the integrity of the original feature space (ScaleKD is not conducted in the frequency space), thus lowering the efficacy of DFM.

E More Visualization Results

In this section, we provide more visualization results for a better understanding of our method. In Figure 5, we provide the frequency distributions of three pre-trained large ViT models. We can observe that these pre-trained ViTs show a consistency in unbalanced frequency distributions: the direct responses are salient and significantly stronger than the alternative responses. And in Figure 6, we show more examples of feature distance distributions of alternative components, comparing scenarios with and without DFM, between the teacher and the student on IN-1K. The results validate DFM can effectively reduce the alternative feature distances between the teacher and the student.

https://doi.org/10.52202/079017-2022

NeurIPS Paper Checklist

1. **Claims**

   Question: Do the main claims made in the abstract and introduction accurately reflect the paper's contributions and scope?

   Answer: [Yes]

   Justification: The abstract and introduction contain three parts: i) motivation, ii) methodology, and iii) experimental results, which are explained in Section 1, Section 2, and Section 3. We discuss the related works in Section 4.

   Guidelines:

   - The answer NA means that the abstract and introduction do not include the claims made in the paper.
   - The abstract and/or introduction should clearly state the claims made, including the contributions made in the paper and important assumptions and limitations. A No or NA answer to this question will not be perceived well by the reviewers.
   - The claims made should match theoretical and experimental results, and reflect how much the results can be expected to generalize to other settings.
   - It is fine to include aspirational goals as motivation as long as it is clear that these goals are not attained by the paper.

2. **Limitations**

   Question: Does the paper discuss the limitations of the work performed by the authors?

   Answer: [Yes]

   Justification: We discuss the limitations in the Conclusion part in our main paper

   Guidelines:

   - The answer NA means that the paper has no limitation while the answer No means that the paper has limitations, but those are not discussed in the paper.
   - The authors are encouraged to create a separate "Limitations" section in their paper.
   - The paper should point out any strong assumptions and how robust the results are to violations of these assumptions (e.g., independence assumptions, noiseless settings, model well-specification, asymptotic approximations only holding locally). The authors should reflect on how these assumptions might be violated in practice and what the implications would be.
   - The authors should reflect on the scope of the claims made, e.g., if the approach was only tested on a few datasets or with a few runs. In general, empirical results often depend on implicit assumptions, which should be articulated.
   - The authors should reflect on the factors that influence the performance of the approach. For example, a facial recognition algorithm may perform poorly when image resolution is low or images are taken in low lighting. Or a speech-to-text system might not be used reliably to provide closed captions for online lectures because it fails to handle technical jargon.
   - The authors should discuss the computational efficiency of the proposed algorithms and how they scale with dataset size.
   - If applicable, the authors should discuss possible limitations of their approach to address problems of privacy and fairness.
   - While the authors might fear that complete honesty about limitations might be used by reviewers as grounds for rejection, a worse outcome might be that reviewers discover limitations that aren't acknowledged in the paper. The authors should use their best judgment and recognize that individual actions in favor of transparency play an important role in developing norms that preserve the integrity of the community. Reviewers will be specifically instructed to not penalize honesty concerning limitations.

3. **Theory Assumptions and Proofs**

   Question: For each theoretical result, does the paper provide the full set of assumptions and a complete (and correct) proof?

https://doi.org/10.52202/079017-2022

Answer: [NA]

Justification: The paper does not include theoretical results

Guidelines:

- The answer NA means that the paper does not include theoretical results.
- All the theorems, formulas, and proofs in the paper should be numbered and cross-referenced.
- All assumptions should be clearly stated or referenced in the statement of any theorems.
- The proofs can either appear in the main paper or the supplemental material, but if they appear in the supplemental material, the authors are encouraged to provide a short proof sketch to provide intuition.
- Inversely, any informal proof provided in the core of the paper should be complemented by formal proofs provided in appendix or supplemental material.
- Theorems and Lemmas that the proof relies upon should be properly referenced.

4. **Experimental Result Reproducibility**

   Question: Does the paper fully disclose all the information needed to reproduce the main experimental results of the paper to the extent that it affects the main claims and/or conclusions of the paper (regardless of whether the code and data are provided or not)?

   Answer: [Yes]

   Justification: We provide all training setups and implementation details in Appendix B

   Guidelines:

   - The answer NA means that the paper does not include experiments.
   - If the paper includes experiments, a No answer to this question will not be perceived well by the reviewers: Making the paper reproducible is important, regardless of whether the code and data are provided or not.
   - If the contribution is a dataset and/or model, the authors should describe the steps taken to make their results reproducible or verifiable.
   - Depending on the contribution, reproducibility can be accomplished in various ways. For example, if the contribution is a novel architecture, describing the architecture fully might suffice, or if the contribution is a specific model and empirical evaluation, it may be necessary to either make it possible for others to replicate the model with the same dataset, or provide access to the model. In general. releasing code and data is often one good way to accomplish this, but reproducibility can also be provided via detailed instructions for how to replicate the results, access to a hosted model (e.g., in the case of a large language model), releasing of a model checkpoint, or other means that are appropriate to the research performed.
   - While NeurIPS does not require releasing code, the conference does require all submissions to provide some reasonable avenue for reproducibility, which may depend on the nature of the contribution. For example
     (a) If the contribution is primarily a new algorithm, the paper should make it clear how to reproduce that algorithm.
     (b) If the contribution is primarily a new model architecture, the paper should describe the architecture clearly and fully.
     (c) If the contribution is a new model (e.g., a large language model), then there should either be a way to access this model for reproducing the results or a way to reproduce the model (e.g., with an open-source dataset or instructions for how to construct the dataset).
     (d) We recognize that reproducibility may be tricky in some cases, in which case authors are welcome to describe the particular way they provide for reproducibility. In the case of closed-source models, it may be that access to the model is limited in some way (e.g., to registered users), but it should be possible for other researchers to have some path to reproducing or verifying the results.

5. **Open access to data and code**

Question: Does the paper provide open access to the data and code, with sufficient instructions to faithfully reproduce the main experimental results, as described in supplemental material?

Answer: [Yes]

Justification: The code has been made publicly available.

Guidelines:

- The answer NA means that paper does not include experiments requiring code.
- Please see the NeurIPS code and data submission guidelines (`https://nips.cc/public/guides/CodeSubmissionPolicy`) for more details.
- While we encourage the release of code and data, we understand that this might not be possible, so "No" is an acceptable answer. Papers cannot be rejected simply for not including code, unless this is central to the contribution (e.g., for a new open-source benchmark).
- The instructions should contain the exact command and environment needed to run to reproduce the results. See the NeurIPS code and data submission guidelines (`https://nips.cc/public/guides/CodeSubmissionPolicy`) for more details.
- The authors should provide instructions on data access and preparation, including how to access the raw data, preprocessed data, intermediate data, and generated data, etc.
- The authors should provide scripts to reproduce all experimental results for the new proposed method and baselines. If only a subset of experiments are reproducible, they should state which ones are omitted from the script and why.
- At submission time, to preserve anonymity, the authors should release anonymized versions (if applicable).
- Providing as much information as possible in supplemental material (appended to the paper) is recommended, but including URLs to data and code is permitted.

6. **Experimental Setting/Details**

   Question: Does the paper specify all the training and test details (e.g., data splits, hyperparameters, how they were chosen, type of optimizer, etc.) necessary to understand the results?

   Answer: [Yes]

   Justification: We detailed explain all experimental settings in Appendix B

   Guidelines:

   - The answer NA means that the paper does not include experiments.
   - The experimental setting should be presented in the core of the paper to a level of detail that is necessary to appreciate the results and make sense of them.
   - The full details can be provided either with the code, in appendix, or as supplemental material.

7. **Experiment Statistical Significance**

   Question: Does the paper report error bars suitably and correctly defined or other appropriate information about the statistical significance of the experiments?

   Answer: [No]

   Justification: The main experiments are conducted on large-scale datasets, whose results are stable.

   Guidelines:

   - The answer NA means that the paper does not include experiments.
   - The authors should answer "Yes" if the results are accompanied by error bars, confidence intervals, or statistical significance tests, at least for the experiments that support the main claims of the paper.
   - The factors of variability that the error bars are capturing should be clearly stated (for example, train/test split, initialization, random drawing of some parameter, or overall run with given experimental conditions).

https://doi.org/10.52202/079017-2022

- The method for calculating the error bars should be explained (closed form formula, call to a library function, bootstrap, etc.)
- The assumptions made should be given (e.g., Normally distributed errors).
- It should be clear whether the error bar is the standard deviation or the standard error of the mean.
- It is OK to report 1-sigma error bars, but one should state it. The authors should preferably report a 2-sigma error bar than state that they have a 96% CI, if the hypothesis of Normality of errors is not verified.
- For asymmetric distributions, the authors should be careful not to show in tables or figures symmetric error bars that would yield results that are out of range (e.g. negative error rates).
- If error bars are reported in tables or plots, The authors should explain in the text how they were calculated and reference the corresponding figures or tables in the text.

8. **Experiments Compute Resources**

   Question: For each experiment, does the paper provide sufficient information on the computer resources (type of compute workers, memory, time of execution) needed to reproduce the experiments?

   Answer: [Yes]

   Justification: We give the demand compute resources in Appendix B

   Guidelines:

   - The answer NA means that the paper does not include experiments.
   - The paper should indicate the type of compute workers CPU or GPU, internal cluster, or cloud provider, including relevant memory and storage.
   - The paper should provide the amount of compute required for each of the individual experimental runs as well as estimate the total compute.
   - The paper should disclose whether the full research project required more compute than the experiments reported in the paper (e.g., preliminary or failed experiments that didn't make it into the paper).

9. **Code Of Ethics**

   Question: Does the research conducted in the paper conform, in every respect, with the NeurIPS Code of Ethics `https://neurips.cc/public/EthicsGuidelines`?

   Answer: [Yes]

   Justification: We have reviewed the code of ethics.

   Guidelines:

   - The answer NA means that the authors have not reviewed the NeurIPS Code of Ethics.
   - If the authors answer No, they should explain the special circumstances that require a deviation from the Code of Ethics.
   - The authors should make sure to preserve anonymity (e.g., if there is a special consideration due to laws or regulations in their jurisdiction).

10. **Broader Impacts**

    Question: Does the paper discuss both potential positive societal impacts and negative societal impacts of the work performed?

    Answer: [Yes]

    Justification: We discuss the broader impacts in Section 6

    Guidelines:

    - The answer NA means that there is no societal impact of the work performed.
    - If the authors answer NA or No, they should explain why their work has no societal impact or why the paper does not address societal impact.
    - Examples of negative societal impacts include potential malicious or unintended uses (e.g., disinformation, generating fake profiles, surveillance), fairness considerations (e.g., deployment of technologies that could make decisions that unfairly impact specific groups), privacy considerations, and security considerations.

- The conference expects that many papers will be foundational research and not tied to particular applications, let alone deployments. However, if there is a direct path to any negative applications, the authors should point it out. For example, it is legitimate to point out that an improvement in the quality of generative models could be used to generate deepfakes for disinformation. On the other hand, it is not needed to point out that a generic algorithm for optimizing neural networks could enable people to train models that generate Deepfakes faster.
- The authors should consider possible harms that could arise when the technology is being used as intended and functioning correctly, harms that could arise when the technology is being used as intended but gives incorrect results, and harms following from (intentional or unintentional) misuse of the technology.
- If there are negative societal impacts, the authors could also discuss possible mitigation strategies (e.g., gated release of models, providing defenses in addition to attacks, mechanisms for monitoring misuse, mechanisms to monitor how a system learns from feedback over time, improving the efficiency and accessibility of ML).

11. **Safeguards**

    Question: Does the paper describe safeguards that have been put in place for responsible release of data or models that have a high risk for misuse (e.g., pre-trained language models, image generators, or scraped datasets)?

    Answer: [NA]

    Justification: The paper poses no such risks.

    Guidelines:

    - The answer NA means that the paper poses no such risks.
    - Released models that have a high risk for misuse or dual-use should be released with necessary safeguards to allow for controlled use of the model, for example by requiring that users adhere to usage guidelines or restrictions to access the model or implementing safety filters.
    - Datasets that have been scraped from the Internet could pose safety risks. The authors should describe how they avoided releasing unsafe images.
    - We recognize that providing effective safeguards is challenging, and many papers do not require this, but we encourage authors to take this into account and make a best faith effort.

12. **Licenses for existing assets**

    Question: Are the creators or original owners of assets (e.g., code, data, models), used in the paper, properly credited and are the license and terms of use explicitly mentioned and properly respected?

    Answer: [Yes]

    Justification: We clearly illustrate the dataset and codebase we use in the Appendix A and the Appendix B, respectively.

    Guidelines:

    - The answer NA means that the paper does not use existing assets.
    - The authors should cite the original paper that produced the code package or dataset.
    - The authors should state which version of the asset is used and, if possible, include a URL.
    - The name of the license (e.g., CC-BY 4.0) should be included for each asset.
    - For scraped data from a particular source (e.g., website), the copyright and terms of service of that source should be provided.
    - If assets are released, the license, copyright information, and terms of use in the package should be provided. For popular datasets, `paperswithcode.com/datasets` has curated licenses for some datasets. Their licensing guide can help determine the license of a dataset.
    - For existing datasets that are re-packaged, both the original license and the license of the derived asset (if it has changed) should be provided.

https://doi.org/10.52202/079017-2022

- If this information is not available online, the authors are encouraged to reach out to the asset's creators.

13. **New Assets**

    Question: Are new assets introduced in the paper well documented and is the documentation provided alongside the assets?

    Answer: [Yes]

    Justification: We obtained some high-performance models in this paper.

    Guidelines:

    - The answer NA means that the paper does not release new assets.
    - Researchers should communicate the details of the dataset/code/model as part of their submissions via structured templates. This includes details about training, license, limitations, etc.
    - The paper should discuss whether and how consent was obtained from people whose asset is used.
    - At submission time, remember to anonymize your assets (if applicable). You can either create an anonymized URL or include an anonymized zip file.

14. **Crowdsourcing and Research with Human Subjects**

    Question: For crowdsourcing experiments and research with human subjects, does the paper include the full text of instructions given to participants and screenshots, if applicable, as well as details about compensation (if any)?

    Answer: [NA]

    Justification: The paper does not involve crowdsourcing nor research with human subjects.

    Guidelines:

    - The answer NA means that the paper does not involve crowdsourcing nor research with human subjects.
    - Including this information in the supplemental material is fine, but if the main contribution of the paper involves human subjects, then as much detail as possible should be included in the main paper.
    - According to the NeurIPS Code of Ethics, workers involved in data collection, curation, or other labor should be paid at least the minimum wage in the country of the data collector.

15. **Institutional Review Board (IRB) Approvals or Equivalent for Research with Human Subjects**

    Question: Does the paper describe potential risks incurred by study participants, whether such risks were disclosed to the subjects, and whether Institutional Review Board (IRB) approvals (or an equivalent approval/review based on the requirements of your country or institution) were obtained?

    Answer: [NA]

    Justification: The paper does not involve crowdsourcing nor research with human subjects.

    Guidelines:

    - The answer NA means that the paper does not involve crowdsourcing nor research with human subjects.
    - Depending on the country in which research is conducted, IRB approval (or equivalent) may be required for any human subjects research. If you obtained IRB approval, you should clearly state this in the paper.
    - We recognize that the procedures for this may vary significantly between institutions and locations, and we expect authors to adhere to the NeurIPS Code of Ethics and the guidelines for their institution.
    - For initial submissions, do not include any information that would break anonymity (if applicable), such as the institution conducting the review.